Bispecific Antibody and Iodine-131-Labeled Bivalent Hapten Dosimetry in Patients with Medullary Thyroid or Small-Cell Lung Cancer

Manuel Bardiès, Stephane Bardet, Alain Faivre-Chauvet, Patrick Peltier, Jean-Yves Douillard, Marc Mahé, Maryse Fiche, Albert Lisbona, Françoise Giacalone, Pascal Meyer, Emmanuel Gautherot, Eric Rouvier, Jacques Barbet and Jean-François Chatal

INSERM Research Unit 211 and Regional Cancer Center, Nantes, France; Immunotech SA, Marseille, France

The purpose of this study was to estimate the dose delivered to tumor targets and normal tissues after two-step injection of an anti-CEA/anti-DTPA-In (F6-734) bispecific antibody and a ^{131}I-labeled di-DTPA In-TL bivalent hapten in patients with medullary thyroid carcinoma (MTC) and small-cell lung cancer (SCLC). **Methods:** Five patients with persistent disease or recurrences of MTC and five patients with primary SCLC or relapse were studied. In a first step, 0.1 to 0.3 mg/kg of F6-734 bispecific antibody was injected intravenously. Four days later, 6 nmole (5.8 to 9.8 mCi) of ^{131}I-labeled di-DTPA In-TL bivalent hapten were injected. Quantitative imaging was performed during one week after the second injection. **Results:** All 5 patients with MTC showed positive immunoscintigraphy (IS). In the smallest visualized and resected tumor (0.8 g), the fraction of injected activity per gram (% ID/g) was 0.1% at Day 3. IS was positive in 4 of the 5 patients with SCLC. The volume of the smallest visualized SCLC tumor was estimated at 11 ± 2 ml, and tumor uptake was about 0.009% ID/g. Tumor dose estimates ranged from 4.2 to 174 cGy/mCi in patients with MTC and from 1.7 to 8 cGy/mCi in patients with SCLC. **Conclusion:** High absorbed dose values were calculated for small MTC recurrences. For SCLC recurrences the values were smaller but in the same range as those obtained by other investigators with the one-step technique in lymphoma.

Key Words: bispecific antibody; two-step targeting; medullary thyroid cancer; small-cell lung cancer

J Nucl Med 1996; 37:1853–1859

Despite the promising results obtained for refractory lymphomas with ^{131}I-labeled monoclonal antibodies (MAbs) (*1,2*), the efficacy of radioimmunotherapy (RIT) with directly labeled antibodies remains limited. Two-step radioimmunotargeting reduces radioactive concentration in normal tissues, thereby increasing tumor-to-normal tissue ratios (*3*). In colorectal carcinoma, tumor-to-blood and tumor-to-liver ratios obtained after two-step injection of nonradiolabeled bispecific anti-carcinoembryonic antigen (CEA)/anti-In-DTPA antibody (BsMAb) and ^{111}In-labeled di-DTPA In-TL bivalent hapten were respectively 1.9- and 3.5-fold higher than those achieved after one-step injection of F(ab')$_2$ fragments of the same ^{111}In-labeled anti-CEA antibody (*4*). Similar results have been obtained in relapses of medullary thyroid cancer (MTC) with the same BsMAb and ^{111}In-labeled bivalent hapten (*5*). These data, extrapolated to ^{131}I, are favorable to RIT application since irradiation of normal tissues with the two-step technique at an equivalent injected activity would be lower than with the one-step technique.

The purpose of this RIT feasibility study in patients with MTC or small-cell lung cancer (SCLC) was to estimate the radiation dose delivered to known tumor targets and normal tissues after two-step injection of a nonradiolabeled anti-CEA/anti-In-DTPA BsMAb and a ^{131}I-labeled di-DTPA In-TL bivalent hapten.

Received Sept. 11, 1995; revision accepted Jan. 28, 1996.

For correspondence or reprints contact: Jean-François Chatal, MD, Research Unit, 211 INSERM, Institut de Biologie, 9 Quai Moncousu, Nantes 44035 Cedex 01, France.

MATERIALS AND METHODS

Patients

The following adult patients were eligible for entry into this study:

1. Patients with measurable persistent disease or local and/or metastatic recurrences of MTC after surgery, as assessed by elevated serum thyrocalcitonin (TCT) concentration and positive morphological imaging techniques, including US and/or CT and/or MRI.
2. Patients with documented primary SCLC or relapse after conventional first-line chemotherapy. Only those patients with CEA-positive immunostaining of primary tumor biopsy specimens, as determined by the immunoperoxidase technique, were eligible. Other eligibility requirements included an absence of chemotherapy and radiotherapy for at least 3 mo. All patients underwent morphological imaging techniques (US, CT or MRI) within 1 mo before injection of BsMAb. All patients gave written informed consent to the protocol, which was approved by the regional ethics committee.

Five patients with MTC and five with SCLC were studied (Table 1). All patients with MTC had undergone total thyroidectomy with removal of regional lymph nodes between 1978 and 1993. At the time of immunoscintigraphy (IS), all five had elevated TCT values, and three had increased CEA values. The extent of the disease varied greatly among the patients (Table 2). Two had a large tumor burden—a mediastinal mass associated with a pulmonary metastasis in Patient 1 and a bulky liver metastasis in Patient 2, whereas cervical or liver recurrences were limited in Patients 3, 4 and 5.

All patients with SCLC except Patient 10 had been treated before IS (chemotherapy associated or not with external-beam radiation). The extent and site of the residual and/or recurrent tumor were variable (Table 2).

Bispecific Antibody Preparation and Bivalent Hapten Iodination

An anti-CEA/anti-In DTPA BsMAb designated as F6-734 (F6-734 BsMAb) was provided by Immunotech Pharma (Marseille, France) with a concentration of 0.68 mg/ml. Briefly, this BsMAb was obtained by coupling an equimolecular quantity of a Fab' fragment of an anti-CEA MAb (F6) to a Fab fragment of an anti-DTPA-indium MAb (734) activated beforehand by a maleimide function.

TABLE 1
Patient Characteristics

Patient no.	Sex	Age (yr)	MTC/SCLC	Previous treatment(s)	TCT (pg/ml)	NSE (ng/ml)	CEA (ng/ml)
1	M	62	MTC	S	24,264	—	107
2	F	48	MTC	S	377,880	—	4712
3	M	46	MTC	S	14,000	—	32
4	F	56	MTC	S	3480	—	5.7
5	M	69	MTC	S, RT	393	—	3.8
6	M	61	SCLC	RT, PCT	—	8.5	2.7
7	M	56	SCLC	RT, PCT	—	9.4	6.9
8	F	60	SCLC	PCT	—	5.7	2.5
9	M	44	SCLC	RT, PCT	—	7.8	22.8
10	M	57	SCLC	none (primary tumor)	—	27	77

MTC = medullary thyroid cancer; SCLC = small-cell lung cancer; S = surgery; RT = radiotherapy; PCT = polychemotherapy; TCT = thyrocalcitonin; NSE = neuron specific enolase; CEA = carcinoembryonic antigen.
Normal ranges: TCT < 10 pg/ml; CEA < 6 ng/ml; NSE < 12 ng/ml.

The bivalent hapten used was N-α-(diethylenetriamine-N,N,N',N''-tetraaceticacid-N''-acetyl)-tyrosyl-Nε-(diethylenetriamine-N,N,N',N'' tetraaceticacid-N''-acetyl) lysine (di-DTPA-TL) obtained by reaction of dianhydride of diethylenetriamine pentaacetic acid (DTPA) with tyrosyl-lysine diacetate (*3*).

The affinity of BsMAb was 4 10^9 M^{-1} to DTPA-indium at 37°C (*3*) and 2.1 10^9 M^{-1} to CEA as measured on LS174T cells (*4*).

Hapten Labeling with Iodine-131

Hapten labeling was performed according to the chloramine-T method. Briefly, 25 μl of a sterile solution of sodium ^{131}I (15.91 GBq/ml or 430 mCi/ml) and 30 μl of a sterile solution of chloramine-T (1 mg/ml) were added to 6 nmole of di-DTPA-TL in which indium had been previously chelated. After a 2-min incubation at room temperature, the oxidation reaction was stopped by addition of 30 μl of a sterile solution of sodium metabisulfite (1 mg/ml). After 5-min incubation, the solution was buffered (pH 5.6) by adding 815 μl of a sterile buffer solution of N-2-hydroxyethyl piperazine N'-2-ethane sulfonic acid (HEPES) 1 M, pH 5.6.

Purification of the ^{131}I-labeled di-DTPA In-TL solution obtained

TABLE 2
Imaging Results

Patient no.	Documented tumor sites	Scintigraphic imaging: Tumor visualization	Tumor uptake at Day 3 (%ID/g)	Tumor effective half-life (hr)	Liver effective half-life (hr)	Kidney effective half-life (hr)
1	Mediastinal mass	†	0.006	68	53	45
	right lung nodule	‡	0.004	51		
2	Liver mass	†	0.003	104	na	na
	right neck lymph nodes	—				
3	3 liver nodules:					
	Segment IV	‡	0.116	119	na	62
	Segment VII	—				
	Segment V	‡	na			
4	Right neck lymph nodes	†	0.108	146	75	89
		†	0.074	73		
5	Right neck lymph node	†	0.100	83	159	84
6	Left lung,	†	0.002	61	na	52
	mediastinal mass	§	0.003	132		
7	Left lung	—			47	35
	3 liver nodules:					
	Segment IV	§	na	na		
	Segment VIII	—				
	Segment VIII	—				
8	Right lung,	†	na	na	48	38
	left lung,	†	na	na		
	adrenal gland*,	—				
	brain	—				
9	Right adrenal gland*,	—				
	left adrenal gland	‡	0.009	80	58	65
10	Left lung (primary tumor)	‡	0.002	47	66	48

*Clinical course did not confirm malignant nature; † highly contrasted; ‡ moderately contrasted; § weakly contrasted.
na = nonassessable.

was performed by reverse-phase chromatography on Sep-Pak C18 cartridges (Waters, Milford, MA). The solution was injected into a cartridge previously conditioned by successive injections of 20 ml of ethanol and 10 ml of sterile HEPES buffer 0.1 *M*, pH 5.6. Free ^{131}I was eliminated in the column by injection of 10 ml of HEPES buffer 0.1 *M*, pH 5.6. The residual buffer contained in the column was then eliminated by successive injections of 1 ml of water and 5 ml of sterile air. The radiolabeled hapten was then eluted by injection of 3 ml of ethanol.

After the purification step, the activities of the ethanolic hapten solution, the buffered solution containing free iodine and the purification cartridge were measured, and the quantity of iodine bound by hapten was estimated from these results and from the specific activity of the ^{131}I solution used for labeling (168.72 TBq/g or 4560 Ci/mg).

The hapten solution was considered to be correctly radiolabeled each time the ratio of the ethanolic solution to the total activity deposited on the purification column was greater than 60%. In these conditions, the mean number of iodine atoms bound per molecule of hapten was estimated as two.

Immunoreactivity

To test the immunoreactivity of ^{131}I-labeled hapten, 5 μl of the ethanolic solution were diluted 1:2000 in buffer (pH 5) containing sodium acetate (100 m*M*), trisodium citrate (10 m*M*) and bovine serum albumin (BSA, 1 g/liter). A volume of 300 μl of this solution was transferred in duplicate into tubes coated with MAb 734 (anti-DTPA-In). After stirring at room temperature for 1 hr, the total activity deposited in each tube was measured in a gamma counter. The tubes were then emptied and washed three times with NaCl/Tween solution. Bound radioactivity was measured again in the same conditions as before. Immunoreactivity, defined as the ratio of bound activity after washing to total deposited activity, was considered satisfactory when the ratio was greater than 80%.

Two-Step Procedure

In a first step, 0.1 to 0.3 mg/kg of nonradiolabeled F6-734 BsMAb was injected by slow intravenous infusion over 20 min (0.09 to 0.1 mg/kg in patients with SCLC and 0.2 to 0.3 mg/kg in those with MTC). After 4 days, 6 nmole of ^{131}I-labeled di-DTPA In-TL (216 to 363 MBq or 5.8 to 9.8 mCi) were injected. Prior to this second injection, patients received 30 drops of Lugol's solution each day, beginning 24 hr before hapten injection and continuing for 3 wk.

Pharmacokinetic Study

Pharmacokinetic analysis was performed according to a methodology previously used, relative to a three-compartmental open model (*6,7*).

All parameters were calculated from this model using appropriate software. Blood samples were drawn before injection of ^{131}I-labeled hapten and then 5, 15, 30 min and 1, 5, 24, 48, 72, 96 and 168 hr after injection. Urine was collected between 0 and 5 hr, 5 and 24 hr and 24 and 72 hr. The radioactivity of blood and urine samples was measured in a gamma counter at Day 7 together with a decay standard. Statistical study of the results (variance analysis) was performed using appropriate software.

Scintigraphic Imaging and Dosimetric Studies

Cumulative activity in whole body, tumor, liver and kidneys was determined by whole-body quantitative scintigraphy performed with a two-headed camera equipped with a high-energy collimator, as proposed by DeNardo et al. (*8*). Whole-body scintigraphic images (anterior and posterior views) were recorded 5 min after injection of ^{131}I-labeled hapten and then at day 1, 2, 3, 4 and 7 using a 20% window set on the ^{131}I photopeak. The positioning of the patient was done in a reproducible manner using a system based on laser sources.

The attenuation corrective factor (ACF) was determined from a transmission image. A collimated linear source perpendicular to the direction of scanning movement was attached to the lower camera head. Acquisition was performed in the presence and then in the absence of the patient on the day of nonradiolabeled F6-734 BsMAb injection, thus defining the geometrical parameters for recordings.

The images were transferred to a Macintosh microcomputer where they were processed using two commercially available programs: Transform (Spyglass, Savoy, IL) and MedVision (Evergreen Technology, Castine, ME). The images acquired in 2048 × 512 format were compressed by summation of pixels to 512 × 128 to provide a format more comparable to the spatial resolution of the high-energy collimator and camera system used. The geometrical mean of each acquisition was calculated and multiplied by the ACF to obtain the resulting image. During each acquisition, a known activity standard was placed at the level of the patient's feet in order to determine the calibration factor for the camera (in counts per MBq in the air).

The activity A(t), in μCi, at each time point t was calculated according to the formula:

$$A(t) = \sqrt{I_{Ant} \cdot I_{Post}} \times ACF \times \frac{f}{C}$$

with

$$ACF = e^{\mu_{eff} L/2} = \sqrt{\frac{I_0}{I}},$$

where I_{Ant} and I_{Post} represent, pixel by pixel, the counts obtained in anterior and posterior views, f the autoattenuation factor of the source (in our study, $f \approx 1$) and C the calibration coefficient for the camera (in counts/μCi). I_0 and I are the counts obtained pixel by pixel on the transmission image in the absence and then the presence of the patient, respectively.

As corrections were performed before regions of interest (ROIs) were defined, the activity on the resulting image was determined by:

$$A(t) = I_{Res}/C,$$

where I_{Res} represents, pixel by pixel, the counts obtained resulting image.

The activities calculated at the different time points were transferred into a pharmacokinetic study program (Siphar, Simed) to determine the effective half-lives of ^{131}I-labeled hapten in the regions defined and then the cumulative activity. In Patients 4 and 5, the activity estimated by quantitative scintigraphy was compared with that of the entire surgically resected tumor measured in a well counter (at Day 7 for Patient 4 and at Day 8 for Patient 5).

The doses absorbed by tumor targets and normal tissues after injection of ^{131}I-labeled hapten were calculated according to the MIRD scheme (*9*). The absorbed dose was defined by:

$$\bar{D}_{(t \leftarrow s)} = \tilde{A} \frac{\Delta \phi_{(t \leftarrow s)}}{m_t},$$

where $\bar{D}_{(t \leftarrow s)}$ is the dose (Gy) delivered to the target t by the source s, $\tilde{A}$ the cumulative activity (MBq.sec or μCi.hr), Δ the constant of the radionuclide dose (g.cGy/μCi.hr) and ϕ the fraction of energy emitted by the source and absorbed by the target mass m_t (g). In the case of ^{131}I and for sources with a diameter greater than 1 cm, ϕ = 1 for beta emissions. Tumor target mass was estimated from CT scan sections with a thickness of 5 mm or 1 cm or, for Patients 4 and 5 determined precisely by weighing the resected tumors.

Dosimetry was performed on scintigraphically visualized tumors for which it was possible to define a target volume (and thus

estimate the mass) from CT scan sections. Due to the partial volume effect, the volumes of the tumors were estimated to have a relative accuracy of 20%. The mass of normal tissues (liver and kidney) was estimated by reference values. ROIs were defined on the liver and left kidney of each patient in order to estimate the doses delivered to these organs.

The calculation of the bone marrow dose was performed according to the technique of De Nardo et al. (*10*) by summing a whole-body component of the bone marrow dose (only penetrating radiations are taken into account) and a blood component (only nonpenetrating radiations are taken into account).

Detection of Anti-Mouse Antibodies

Anti-mouse antibodies (HAMA) were assessed according to a previously described procedure (*4*). Briefly, human anti-bispecific antibody concentration was determined in duplicate from patients' sera using a one-step double antigen sandwich radioimmunoassay on F6-734 BsMAb-coated tubes.

RESULTS

Hapten Labeling

The di-DTPA In-TL hapten labeling technique was reproducible. Labeling efficiency showed little variation (between 60% and 68%), and immunoreactivity ranged from 91% to 99%.

Tumor Imaging

All patients with MTC had positive IS results (Table 2). Tumors were clearly visualized at 24 hr in patients with various TCT and/or CEA serum concentrations, various localizations and various burdens, but contrast was increased at Days 5 or 7 due to a reduction in adjacent nonspecific activity (Fig. 1). Relative to conventional morphological imaging, IS visualized an additional tumor site in Patient 4 who underwent surgery after IS (Fig. 2). The smallest visible tumor (a right neck lymph node resected in Patient 5) weighed 0.8 g.

IS was clearly positive in four of the five SCLC patients but all documented tumor sites were not visualized in two of these four patients; for Patient 6, a large hot spot was visualized early in the left lung (at Day 0), and high contrast was observed from Days 3 to 7. This large tumor, later confirmed by CT scan, was estimated to weigh about 125 g. An additional mediastinal mass, not previously documented, was visualized on an IS anterior planar view and subsequently confirmed by CT from which volume could be estimated. IS was falsely negative for Patient 7 in three documented tumor sites and weakly positive in a small liver metastasis. For Patient 8, IS was clearly positive in a large recurrence infiltrating both lungs, but the volume could not be even roughly estimated on CT. For the same patient, IS failed to visualize cerebral metastases and hypertrophic adrenal glands. Under polychemotherapy, lung tumors regressed in size, whereas the hypertrophic adrenal glands remained unchanged (presumably nonmetastatic). For Patient 9, IS imaged one (left) of the enlarged adrenal glands visualized on CT (Fig. 3). Under polychemotherapy the left adrenal tumor regressed in size, whereas no change occurred in the right adrenal mass (presumably nonmetastatic).

Pharmacokinetic Study

The results of the pharmacokinetic study are reported in Table 3. Mean distribution half-lives ($T_{1/2}$ α, β and γ) and mean residence time for all 10 patients were 0.50 ± 0.24 hr, 7.71 ± 2.95 hr and 63.72 ± 21.68 hr, respectively. The corresponding pre-exponential values (mCi/liter) were 0.376 ± 0.096, 0.185 ± 1.196 and 1.184 ± 0.345, respectively. Mean residence time for all 10 patients was 66.66 ± 13.40 hr. Two of the 10 patients (Patients 4 and 7) presented pharmacokinetic parameters which could only be analyzed using a two-compartmental open model.

Values for equilibrium distribution volume, elimination half-lives and clearances (blood and urine) in patients with MTC (injected BsMAb: 0.3 mg/kg) and SCLC (injected BsMAb: 0.1 mg/kg) were significantly different: 14.89 ± 7.71 l versus 64.01 ± 31.54 l ($p < 0.01$); 49.63 ± 13.73 versus 77.82 ± 19.28 hr ($p < 0.03$); 0.27 ± 0.18 $l \cdot hr^{-1}$ versus 0.90 ± 0.46 $l \cdot hr^{-1}$ ($p < 0.02$) and 0.21 ± 0.17 $l \cdot hr^{-1}$ versus 0.74 ± 0.24 $l \cdot hr^{-1}$ ($p < 0.004$), respectively.

The mean fraction (±s.d.) of activity excreted in urine was 20.7 ± 9.0% from 0 to 5 hr, 20.2 ± 5.1% from 5 to 24 hr and 12.9 ± 6.1% from 24 to 72 hr in patients with MTC, and 45.4 ± 4.0% from 0 to 5 hr, 25.0 ± 5.0% from 5 to 24 hr and 5.7 ± 3.6% from 24 to 72 hr in patients with SCLC.

Dosimetric Studies

The results for dosimetric studies are shown in Table 4. The dosimetric approach was validated on a phantom by determining the optimal protocol for quantitative scintigraphy. Real activity was assessed in spherical sources of different volume (0.5 to 10 ml) simulating tumors or in sources of greater volume simulating organs (150-ml container of physiological serum simulating a kidney, 3-liter cylinder simulating a liver) immersed in an oval 15-liter tank, with or without background noise, simulating the abdominal cavity.

The ACF was calculated for each patient. The correction for each image pixel varied between 1.5 and 3 according to the patient and the anatomical regions considered.

The activity in each ROI was determined from the standard source positioned in the air next to the patient during acquisition, except for whole-body activity, which was determined from the percentage of counts obtained 10 min after injection on Day 0, taken as the reference. As reported in Table 2, tumor effective half-lives ranged from 51 to 146 hr for MTC patients and from 47 to 132 hr for SCLC patients. Liver and kidney effective half-lives ranged from 53 to 159 hr and 45 to 89 hr for MTC patients and from 47 to 66 hr and 35 to 65 hr for SCLC patients, respectively. The results for tumor uptake, expressed in %ID/g at Day 3, as a function of tumor mass, are shown in Figure 4. It is quite apparent that tumor uptake was much higher (on an order of magnitude) for small tumors weighing about 1 g than for those weighing more than 10 g.

For three small nodules, activities obtained by quantitative imaging were compared with those obtained by counting resected tumors. For Patient 4, the activity in two right neck lymph nodes (weighing 1.15 g and 0.83 g as assessed after resection) was 5.1 and 2.7 μCi at Day 7, respectively. Activities calculated at Day 6 from quantitative imaging were 6.4 and 3 μCi, respectively. For Patient 5, the activity in a right neck lymph node (0.80 g as assessed after resection) was 3.3 μCi at Day 8. Activity calculated at Day 7 from quantitative imaging was 4.1 μCi. This good agreement validates our quantitative imaging protocol.

For patients with MTC, tumor-to-blood ratios ranged from 0.6 to 69.1 (Fig. 5). If we exclude the 0.6 value (Patient 2), attributable to a very elevated serum CEA concentration leading to the formation of radioactive immune complexes, the mean value was 41. Tumor-to-liver ratios ranged from 7.6 to 125.5 (mean: 51), and tumor-to-kidney ratios from 1.4 to 39.4 (mean: 13). For patients with SCLC, tumor-to-blood ratios ranged from 3.4 to 18.8 (mean: 11), tumor-to-liver ratios from 8.1 to 14.5 (mean: 8.4) and tumor-to-kidney ratios from 0.2 to 6.5 (mean: 2.7).

For tumor targets, absorbed doses ranged between 1.7 cGy/

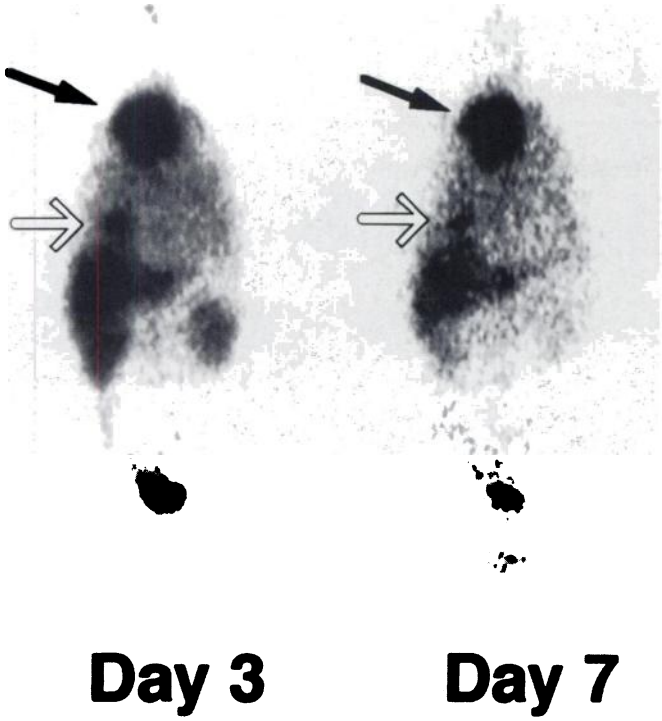

FIGURE 1. Whole-body anterior views of Patient 1 obtained 3 and 7 days after injection of ^{131}I-labeled hapten (7 and 11 days after a first injection of BsMAb). Clear visualization of a 125 cm^3 mediastinal recurrence (closed arrow) and a 10 cm^3 right lung metastasis (open arrow).

mCi for Patient 10 with a primary tumor and 174 cGy/mCi for Patient 3 with a liver metastasis (Table 4).

To calculate the doses delivered to the liver and left kidney, the contours of these organs were sketched on the images, except when the liver was indistinguishable from liver metastases (Patients 2 and 3) or when high circulating activity prevented clear imaging of the kidney (Patient 2). Doses were calculated by

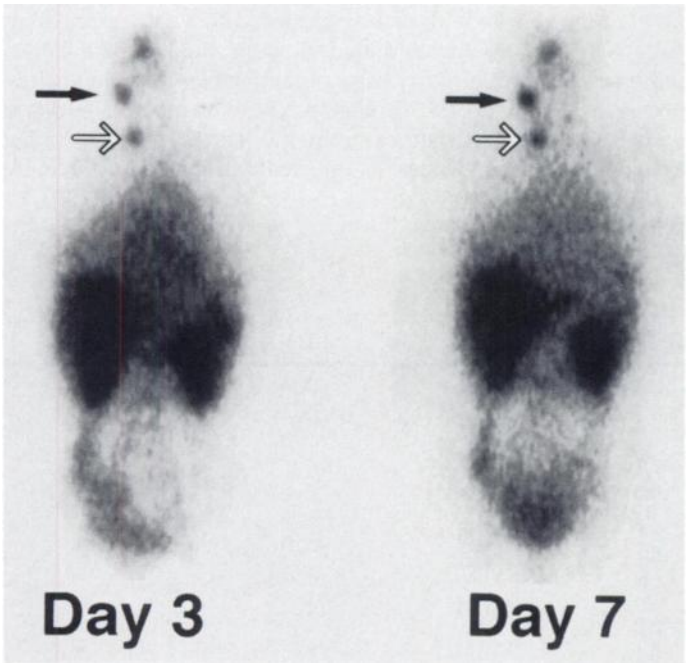

FIGURE 2. Whole-body anterior views of Patient 4 obtained 3 and 7 days after injection of ^{131}I-labeled hapten (7 and 11 days after a first injection of BsMAb). Highly contrasted visualization of two 1.15 g (closed arrow) and 0.83 g (open arrow) right neck recurrences surgically resected 7 days after hapten injection.

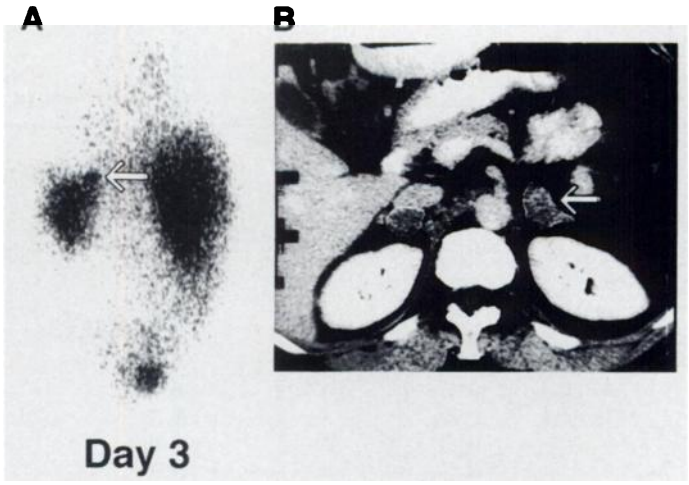

FIGURE 3. (A) Posterior abdominal view of Patient 9 obtained 3 days after injection of ^{131}I-labeled hapten (7 days after a first injection of BsMAb). A hot spot is visualized in the left suprarenal area (open arrow). (B) Abdominal CT scan shows bilateral adrenal masses. Left adrenal mass (open arrow) has a 11 ± 2 cm^3 volume.

assuming a mean mass of 1800 g for the liver and 120 g for the kidney. Doses between 0.2 and 4.3 cGy/mCi were computed for liver and between 1.3 cGy/mCi and 9 cGy/mCi for kidney.

Bone marrow absorbed doses, calculated from sketched contours (whole-body component) and results of blood kinetics, were between 0.2 and 1.5 cGy/mCi. Blood absorbed doses ranged between 0.1 and 1.1 cGy/mCi.

Detection of Anti-Mouse Antibodies

HAMA was positive for three of the five patients with MTC: One early detection 15 days after BsMAb injection (Patient 5) and two later detections at day 90 (Patients 1 and 3). HAMA was positive during the first month after BsMAb injection in two of the five patients with SCLC.

DISCUSSION

The results of this study confirm those previously obtained with the same BsMAb and ^{111}In-labeled bivalent hapten, showing favorable tumor uptake values and tumor-to-normal tissue ratios for RIT applications. In patients with colorectal carcinomas, tumor uptake values were the same for the one- and two-step techniques, but tumor-to-blood and tumor-to-liver ratios were 1.9- to 3.5-fold higher with the latter technique (*4*). In the same clinical situation of colorectal carcinoma, very high tumor uptake values (greater than 0.1% ID/g), comparable to those for MTC patients in our study, have been found when an anti-CEA antibody directly labeled with ^{131}I was used for small tumor targets of less than 10 g (*11*). For MTC patients in the present study, tumor-to-normal tissue ratios were above 50 in two patients and above 10 in six. The only value below 1 was obtained in Patient 2 with a tumor mass weighing 500 g and a very high serum CEA concentration. In comparison, two studies (concerning a limited number of patients) have reported tumor-to-normal tissue ratios lower than 5 when an anti-CEA antibody directly labeled with ^{111}In was used (*12,13*).

In our study, a three-compartmental open model appeared to be the most suitable choice for pharmacokinetic analysis, in accordance with theoretical data published by Baxter et al. (*7*) and comments concerning the limitations of a two-compartmental model (*6*). Based on data reported by Le Doussal et al. (*4*), who used the same BsMAb and the same ^{111}In-labeled hapten, we found shorter distribution half-lives than those obtained when a directly labeled antibody was used (less than 30 min on average

TABLE 3
Pharmacokinetic Analysis According to a Three-Compartment Model

Patients	$T_{1/2}\ \alpha$ (hr)	$T_{1/2}\ \beta$ (hr)	$T_{1/2}\ \gamma$ (hr)	VDss (l)	MRT (hr)	Blood cl. ($l \cdot hr^{-1}$)	Urin. cl. ($l \cdot hr^{-1}$)	AUC ($mCi \cdot hr \cdot l^{-1}$)
MTC								
1	0.79	11.78	65.57	28.06	48.82	0.57	0.49	13.27
2	0.84	9.53	60.81	7.74	84.60	0.09	0.05	97.90
3	0.22	3.26	45.78	12.75	63.72	0.20	0.17	22.95
4	0.68	—	31.29	13.75	43.86	0.31	0.22	22.01
5	0.12	3.89	44.70	12.16	62.24	0.19	0.11	40.70
mean	0.53	7.11	49.63	14.89	60.65	0.27	0.21	39.36
$\pm\sigma$	±0.33	±4.20	±13.73	±7.71	±15.87	±0.18	±0.17	±34.21
SCLC								
6	0.40	6.46	88.41	110.52	70.88	1.56	0.84	4.77
7	0.60	—	59.75	26.05	85.27	0.30	0.31	22.14
8	0.40	9.40	106.28	73.35	74.64	0.98	0.84	7.90
9	0.37	8.26	64.26	47.03	66.21	0.71	0.76	11.56
10	0.62	9.10	70.42	63.12	66.42	0.95	0.93	9.02
mean	0.48	8.30	77.82	64.01	72.68	0.90	0.74	11.08
$\pm\sigma$	±0.12	±1.32	±19.28	±31.54	±7.85	±0.46	±0.24	±6.64

MTC = medullary thyroid cancer; SCLC = small-cell lung cancer; VDss = steady-state distribution volume; MRT = mean residence time; cl = clearance; AUC = area under the curve; ns = nonsignificant.

for the two-step system in our study versus more than 2 hr for a directly labeled antibody (*14,15*)). The elimination kinetics study showed no significant differences between the one- and two-step systems. The mean residence times found in our study show that the values obtained are close to those for elimination half-lives. This would seem to confirm that the radioactivity elimination step after injection of ^{131}I-labeled hapten is limited owing to the elimination of circulating hapten-BsMAb complexes.

Studies were conducted on a phantom to validate the dosimetric protocol. The effect of patient volume on photon scatter and quantification of activity present in tumor and normal tissues was studied for increasing source volumes (unpublished data). The results show that error during determination of the activity present in small sources (0.5 to 10 ml) was low (less than 10%) but could be high for large volumes (up to 200% for an oval 15-liter abdominothoracic phantom 22 cm thick). As total activity measurements were available for the tumors of Patients 4 and 5 after surgery. These results were compared with those obtained from scintigraphic images recorded before the operation and found to be in close agreement. It should be noted, however, that background activity subtraction was easier on late images, thus augmenting the accuracy of activity calculations.

Background noise before subtraction was estimated for each ROI based on the minimal count value in this zone. As the definition of a ROI is highly operator-dependent, all zones were sketched by the same persons (a physician assisted by a physicist). In these conditions, even though the precision of the calculated activity may be debatable, we sought to minimize operator-related differences between patients.

In the clinical situation of MTC, recurrences of tumor uptake values were correlated with the volume of the targets considered (Fig. 4), reaching a maximum value of 0.116 %ID/g at day three (Patient 3). These elevated tumor uptake values for small targets, which are comparable to those calculated by Siegel et al. (*11*) in patients with recurrences of colorectal cancer, may have been due to higher blood flow in smaller than larger tumors. Vaupel et al. (*16*) have in fact shown that blood flow decreases exponentially in relation to tumor mass. The doses delivered to tumors ranged from 4.2 to 174 cGy/mCi. By extrapolating these values to injected activities of 100 mCi,

TABLE 4
Dosimetric Calculations

Patient no.	Tumor mass (g)	Dose (cGy/mCi)					
		Tumor	Liver	Left kidney	Blood	(TR)	Bone marrow
1	125.0	4.8	0.5	2.6	0.3	(4.5)	0.5
	10.0	5.3				(5.0)	
2	500.0	4.2	na	na	1.1	(0.9)	1.5
3	1.8	174	na	8.1	0.3	(143.8)	0.6
4	1.15	125	1.1	9.0	0.3	(95.9)	0.6
	0.83	74				(56.5)	
5	0.80	135	4.3	2.5	0.5	(63.1)	0.9
6	315.0	1.9	0.5	1.6	0.07	(6.7)	0.2
	15.0	3.9				(13.7)	
7	—	—	0.3	2.9	0.2		0.4
8	—	—	0.2	5.1	0.1		0.2
9	12.0	8.0	0.4	1.3	0.2	(13.1)	0.3
10	40.0	1.7	0.4	6.1	0.1	(3.8)	0.2

na = nonassessable; TR = therapeutic ratio; $\tilde{C}_{Tumor}$ (μCi·hr/g)/$\tilde{C}_{Blood}$ (μCi·hr/ml).

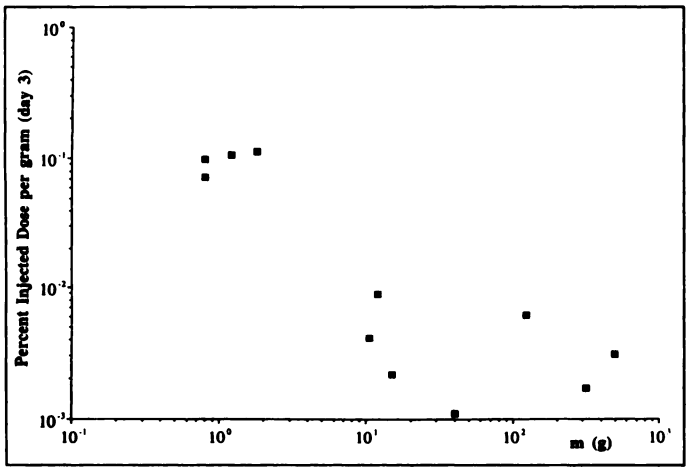

FIGURE 4. Tumor uptake (%ID/g) 3 days after injection of ^{131}I-labeled hapten versus tumor weight.

comparable to the activity of ^{131}I administered for treatment of metastases of differentiated thyroid carcinoma, absorbed tumor doses of 135 and 174 Gy would be obtained for a cervical metastasis of 0.8 g (Patient 5) and a liver metastasis of 1.8 g (Patient 3), respectively. Much lower doses (less than 10 Gy) would be delivered to large tumors (Patients 1 and 2). Thus, these results confirm the commonly accepted opinion that RIT is maximally efficient for small tumors, particularly micrometastases (*17*). The potential interest of this approach can be evaluated relative to the clearly established use of internal radiotherapy with ^{131}I for metastases of differentiated thyroid carcinoma, even though the radiosensitivity of the two types of cancer is not the same. The absorbed tumor dose values computed in this study are comparable to those reported by Thomas et al. (*18*) for cervical metastases (43 to 140 cGy/mCi for tumors weighing 8 to 40 g).

In the clinical situation of SCLC recurrences, tumor uptake values were much lower than for MTC recurrences, reaching a maximum value of 0.009 %ID/g for a tumor weighing about 12 g (Patient 9). Although patients were included in the study on the basis of CEA expression by cells of their primary tumor, as evaluated by immunohistochemical analysis of biopsy material, it is possible that the recurrences themselves expressed less CEA, which could account for the relatively low tumor uptake values. Moreover, tumor volume was generally higher, and the mean quantity of BsMAb injected was one-third of that

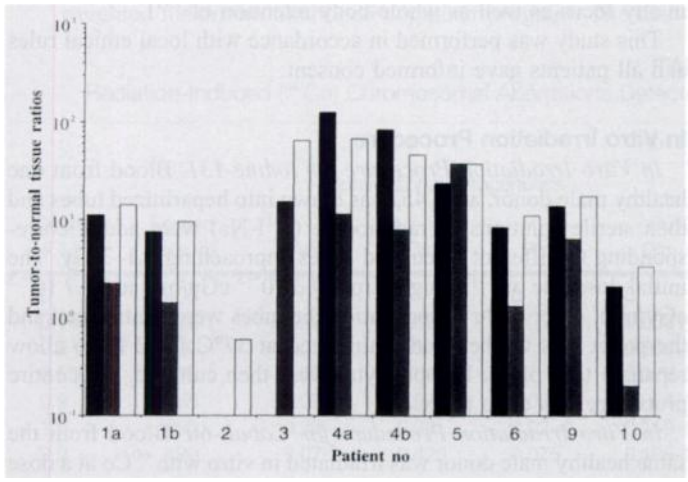

FIGURE 5. Tumor-to-normal tissue ratio as determined by quantitative scintigraphy: tumor-to-liver (black), tumor-to-kidney (gray), tumor-to-blood (white).

administered to patients with MTC, which could also account for the lower uptake values. Irradiation doses, estimated between 1.9 and 8 cGy/mCi in the 5 patients, are comparable to those estimated for a variety of ^{131}I-labeled antibodies in patients with refractory forms of lymphoma presenting radiosensitivity comparable to that of SCLC (*19–21*).

CONCLUSION

A two-step pretargeting system using anti-CEA/anti-DTPA indium BsMAb and a ^{131}I-labeled di-DTPA In-TL bivalent hapten allowed us to obtain high tumor uptake and absorbed dose values for small MTC recurrences. For SCLC recurrences, the values of the same parameters were lower but in the same range as those obtained by other investigators with the one-step technique in refractory lymphoma.

ACKNOWLEDGMENT

This work was supported by a grant from the Programme Hospitalier de Recherche Clinique 1994 conducted by the French Ministry of Health.

REFERENCES

1. Kaminski MS, Zasadny KR, Francis IR, et al. Radioimmunotherapy of B-cell lymphoma with [^{131}I]-anti-B1 (anti-CD 20) antibody. *N Engl J Med* 1993;329:459–465.
2. Press OW, Eary JF, Appelbaum FR, et al. Radiolabeled-antibody therapy of B-cell lymphoma with autologous bone marrow support. *N Engl J Med* 1993;329:1219–1224.
3. Le Doussal JM, Gruaz-Guyon A, Martin M, et al. Targeting of indium-111-labeled bivalent hapten to human melanoma mediated by bispecific monoclonal antibody conjugates: imaging of tumors hosted in nude mice. *Cancer Res* 1990;50:3445–3452.
4. Le Doussal JM, Chetanneau A, Gruaz-Guyon A, et al. Bispecific monoclonal antibody mediated targeting of an indium-111-labeled DTPA dimer to primary colorectal tumors: pharmacokinetics, biodistribution, scintigraphy and immune response. *J Nucl Med* 1993;10:1662–1671.
5. Peltier P, Curtet C, Chatal JF, et al. Radioimmunodetection of medullary thyroid cancer using a bispecific anti-CEA/anti-Indium-DTPA antibody and an indium-111-labeled DTPA dimer. *J Nucl Med* 1993;34:1267–1273.
6. Yuan F, Baxter LT, Jain RK. Pharmacokinetic analysis of two-step approaches using bispecific and enzyme-conjugated antibodies. *Cancer Res* 1991;51:3119–3130.
7. Baxter LT, Yuan F, Jain RK. Pharmacokinetic analysis of the perivascular distribution of bispecific antibodies and haptens: comparison with experimental data. *Cancer Res* 1992;52:5838–5844.
8. DeNardo GL, DeNardo SJ, Macey DJ, et al. Quantitative pharmacokinetics of radiolabeled monoclonal antibodies for imaging and therapy in patients. In: Srivastava SC, ed. *Radiolabeled monoclonal antibodies for imaging and therapy*. New York: Plenum; 1988:293–309.
9. Loevinger R, Budinger TF, Watson EE. MIRD primer for absorbed dose calculations. Society of Nuclear Medicine, 1988.
10. DeNardo GL, Mahé MA, DeNardo SJ, et al. Body and blood clearance and marrow radiation dose of ^{131}I-Lym-1 in patients with B-cell malignancies. *Nucl Med Com* 1993;14:587–595.
11. Siegel JA, Pawlyk DA, Lee RE, et al. Tumor, red marrow and organ dosimetry for ^{131}I-labeled anti-carcinoembryonic antigen monoclonal antibody. *Cancer Res* 1990; 50:1039s–1042s.
12. Reiners C, Eilles C, Spiegel W, et al. Immunoscintigraphy in medullary thyroid cancer using an ^{123}I- or ^{111}In-labeled monoclonal anti-CEA antibody fragment. *J Nucl Med* 1986;25:227–231.
13. Edington HD, Watson CG, Levine G, et al. Radioimmunoimaging of metastatic medullary carcinoma of the thyroid gland using an indium-111-labeled monoclonal antibody to CEA. *Surgery* 1988;104:1004–1010.
14. Hnatowich DJ, Gionet M, Rusckowski M, et al. Pharmacokinetics of ^{111}In-labeled OC-125 antibody in cancer patients compared with the 19-9 antibody. *Cancer Res* 1987;47:6111–6117.
15. Kinuya S, Jeong JM, Garmestani K, et al. Effect of metabolism on retention of Indium-111-labeled monoclonal antibody in liver and blood. *J Nucl Med* 1994;35: 1851–1857.
16. Vaupel P. Oxygen supply to malignant tumors. In: Petersen HI, ed. *Tumor blood circulation: angiogenesis, vascular morphology and blood flow of experimental and human tumors*. Boca Raton: CRC Press; 1979:143.
17. Zanzonico P. Radioimmunotherapy of micrometastases: a continuing evolution. *J Nucl Med* 1992;33:2180–2183.
18. Thomas SR, Maxon HR, Kereiakes JG, et al. Quantitative external counting techniques enabling improved diagnostic and therapy decisions in patients with well-differentiated thyroid cancer. *Radiology* 1977;122:731–737.
19. Eary JF, Press OW, Badger CC, et al. Imaging and treatment of B-cell lymphoma. *J Nucl Med* 1990;31:1257–1268.
20. Goldenberg DM, Horowitz JO, Sharkey RM, et al. Targeting, dosimetry and radioimmunotherapy of B-cell lymphoma with iodine-131-labeled LL2 monoclonal antibody. *J Clin Oncol* 1991;9:548–564.
21. Kaminski MS, Fig LM, Zasadny KR, et al. Imaging, dosimetry and radioimmunotherapy with iodine-131-labeled anti-CD 37 antibody in B-cell lymphoma. *J Clin Oncol* 1992;10:1696–1711.